International Journal on Advanced Science Engineering Information Technology

Vol.12 (2022) No. 4
ISSN: 2088-5334

Tuning of Extended-Resonance-Based Beamforming System for Visible Light Communication

Herminarto Nugroho [a,*], Muhammad Akbar Barrinaya [b]

[a] Department of Electrical Engineering, Universitas Pertamina, Jakarta, 12220, Indonesia
[b] Department of Mechanical Engineering, Universitas Pertamina, Jakarta, 12220, Indonesia
Corresponding author: *herminarto.nugroho@universitaspertamina.ac.id

***Abstract*— Visible Light Communication (VLC) uses the visible light emitted from Light Emitting Diode (LED) to transmit/receive data. Since the data is transmitted through the light, the connection speed is as fast as the speed of light, making it potential for very fast and massive data exchange. One thing that needs to be considered in VLC is that the power of the signal received by the sensor relies on the angle between the LED and the light sensor used as an antenna. The bigger the angle between LED and light sensor, the less optimal the signal power will be, and surely will affect the speed and reliability of the data transmission. To optimize the signal power, multiple photonic sensors will be used as an antenna to receive the light signal. The signal received from each photonic sensor will be combined to get higher signal power. However, to ensure that all signals from all photonic sensors are constructive to each other, all phase differences must be minimized. This paper proposes the extended-resonance-based beamforming system to be used to minimize the phase difference of the light signals in VLC application. A non-linear optimization method is used to tune the extended-resonance-based beamforming system. Given that the varactor is chosen carefully and sufficient enough, the non-linear optimization method such as active set, interior point, or sequential quadratic programming is able to tune the varactor, so that the beamformer will compensate the phase difference from the incoming signal.**

***Keywords*— Visible light communication; extended-resonance; beamforming; non-linear optimization.**

Manuscript received 17 Feb. 2021; revised 29 Jun. 2021; accepted 26 Nov. 2021. Date of publication 31 Aug. 2022.

I. INTRODUCTION

Light Emitting Diode (LED) light nowadays is the most used source of light in houses, offices, roads, and other places as well. This is based on the fact that LED light has much higher efficiency than light bulbs [1]. Other advantages of LED lights are long-lasting, lower heat energy produced, and able to emit some different intensities of light with high frequency [1]. All these advantages motivate the development of a high-speed communication technology using visible light from the LED, which is called Visible Light Communication (VLC) [2],[3]. Moreover, since the LED light is an electromagnetic wave with a frequency that cannot go through walls or any other solid surfaces, the security of the data transfer through VLC can be secured [4]–[6].

Signal transmission in VLC system uses LED a driver controller circuit controls light witch. This controller regulates the current going to the LED. Therefore, the intensity of the LED light can be a controller as we want [4]. By using this controlled light intensity, we can transmit a signal. For example, we can transmit a high and low signal by controlling two light intensities emitted by LED. The sensors that can be used to receive the light signal are photodetector and imaging sensor. Photodetector is a semiconductor device which is able to convert light energy to electric energy. Meanwhile, imaging sensor is an array of small photodetectors which is constructed to a certain geometry. This imaging sensor usually is applied in the CMOS camera sensor [7]–[9].

In the transmission process, there are sone factors which affect the power of the signal received by the light sensor/antenna. Those factors are the distance between LED and sensor/antenna, the angle of transmission from LED, and the angle of reception of the sensor/antenna. The illustration of those factors can be observed in Fig. 1.

Mathematically, the power loss from the signal transmission, which is called path loss (L_L) is represented by the following Equation:

$$L_L = \frac{(m+1)A_r}{2\pi D^2}\cos(\alpha)\cos^2(\beta), \quad (1)$$

where β is the angle of transmission from LED, α is the angle of reception of the sensor, D is the distance between the LED and the sensor, and m is the order of Lambertial emission. Those three factors depend on the sensor's position, and orientation relative to the LED as the light source. The power of the signal will be maximum when the sensor is located exactly below the LED. However, the sensor position is not exactly below the LED, so the signal's power is not optimal as well.

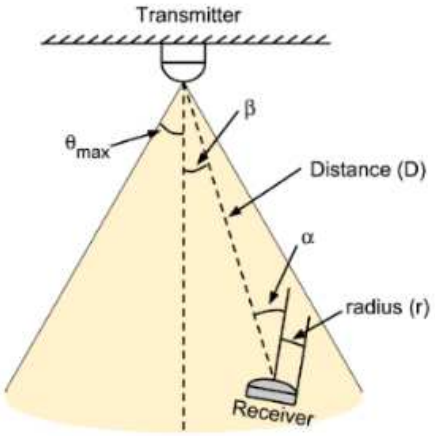

Fig. 1 The illustration of the factors that affect the power of the light signal received by the light sensor [4].

In order to increase the power of the signal, a multi-photodetector sensor is used as an antenna. This type of sensor consists of some photodetectors which are combined in an array antenna configuration. Each photodetector will receive the light signal that comes from the LED. Then, the output of each photodetector will be combined. Therefore, hopefully, the total power from the combined output will be bigger. However, if the phase of the combined signals is not the same, the total power of the signal will not be constructive to each other. The phase of the combined signals depends on the angle of the incoming light signal. When the light signal is coming from a certain angle, each of the sensors/antennae will receive a light signal with a certain time delay from each other.

In order to correct the phase difference between signals received by each antenna/sensor, a beamforming system is needed. Some previous research has been conducted to correct the phase difference in Phased Array Antennas (PAAs) using Optical Beamforming Networks (OBFNs) [10], [11]. The OBFN system uses Optical Ring Resonator (ORR) as a delay element to control the phase of each signal [12], [13]. This beamforming is categorized as analog beamforming [14]–[16]. However, there is a disadvantage of using ORR as a delay element. To understand the disadvantage of ORR, observe the Equation of the delay time produced by ORR for a specific frequency bellow:

$$\tau(f) = \frac{\kappa T}{2 - \kappa - 2\sqrt{1-\kappa}\cos(2\pi f T + \phi)}, \qquad (2)$$

where κ, ϕ, T define the coupling coefficient, extra phase shift, and round-trip period of an ORR, respectively. There is a trade-off between the delay time that ORR can produce and the frequency range it operates. The higher the frequency of the signal, the lower the delay time ORR can produce. Some research of OBFN with ORR as delay element is conducted for the signal is the GHz frequency range. However, the VLC uses visible light in 400-700 THz spectrum. In order to increase the delay time for a higher frequency, we should use an ORR with a bigger round-trip period (T) [17]. Because of bigger T, the dimension of the ORR will become bigger as well, this is not desirable.

An alternative beamforming system is the extended-resonance-based beamforming system [18]. This beamforming is based on the extended-resonance power-dividing method. This method eliminates the need for extra phase shifters in conventional beamforming and reduces the beamformer's cost, complexity, and dimension. This extended-resonance-based beamforming system is proposed to correct the phase difference in the VLC system. In order to tune the extended-resonance beamforming system, we used the non-linear optimization method. In this paper, the tuning simulation, extended-resonance beamforming system, and the simulation setup are presented

II. Materials and Method

The basic concept and the design of the extended-resonance beamforming technique is presented in [13], [14]. This paper will implement the modified approach of the extended-resonance beamforming technique with improved performance, which is presented in [12]. The design of the extended-resonance beamforming is depicted in Figure 2.

The concept of the extended-resonance beamforming is based on the power-divider ports which are connected to an antenna with a certain antenna gain (G_{ant}). The power-divider ports are connected to antenna in shunt with a variable capacitor (varactor). This varactor is tunable in order to transform the admitance to its complex conjugate, i.e.

$$(nG_{ant} + nj\omega C) \rightarrow (nG_{ant} - nj\omega C). \qquad (3)$$

where n is the port number, G_{ant} is the antenna gain, ω is the angular frequency of the signal, and C is the value of the varactor.

The value of the inductance L_n depends on the value of the variable capacitor. In order to transform the admittance as shown in Equation (3), the value of the inductance L_n should be

$$L_n = \frac{2C}{n(G_{ant}^2 + \omega^2 C^2)}. \qquad (4)$$

By setting the value of the inductor as mentioned in Equation (4), the voltage ratio in each successive port will be equal to

$$\frac{V_{n+1}}{V_n} = \frac{(G_{ant} + j\omega C)^2}{G_{ant}^2 + \omega^2 C^2}. \qquad (5)$$

From Equation (5), one can derive the phase difference between two successive ports as follow:

$$\phi_{n+1,n} = \angle\frac{V_{n+1}}{V_n},$$
$$\phi_{n+1,n} = \tan^{-1}\left(\frac{2\omega C G_{ant}}{G_{ant}^2 - \omega^2 C^2}\right). \qquad (6)$$

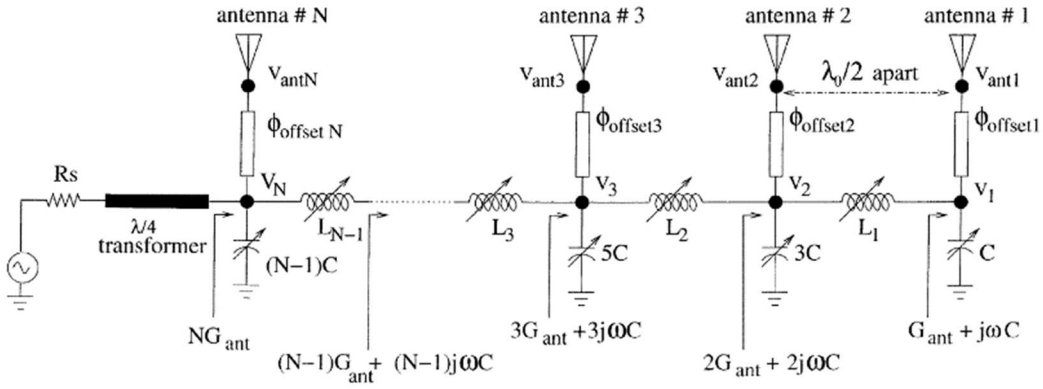

Fig. 2 The one-dimensional extended-resonance-based beamforming system [18]

From Equation (6) we can tune the value of the varactor to obtain the desired phase shift, such that it can compensate the phase difference from the light signal received by each antenna/sensor.

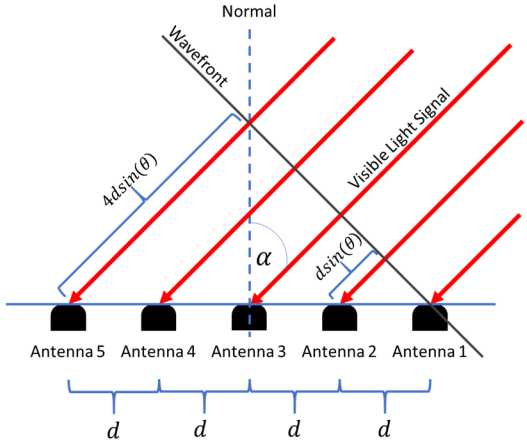

Fig. 3 Illustration of antenna configuration and the angle of the visible light signal.

Consider a one-dimensional antenna configuration and the visible light signal coming from a certain angle (α) relative to the normal of the antenna, as illustrated in Fig. 3. Each antenna will receive a delayed version of the visible light signal depending on the position. For example, in Fig. 3, antenna 1 will receive the light signal the first time, and antenna 2-5 will receive the delayed version of the signal received by antenna 1. Consider d is the distance between antenna and c is the speed of light, the time delay of the light signal for two successive antenna is derived as

$$\tau_{n+1,n} = \frac{d\,sin(\alpha)}{c}, \tag{7}$$

where n is the index of the antenna?

The relationship between phase (ϕ) and delay (τ) is given by

$$\tau = -\frac{1}{2\pi}\frac{\partial\phi}{\partial f}, \tag{8}$$

and therefore, we can obtain the phase difference between two successive antennas created by the delay time of the light signal as

$$\phi_{n+1,n} = -2\pi f \tau_{n+1,n}. \tag{9}$$

One can derive the relationship between the time delay of two successive antennas with the value of varactors by substituting Equation (9) into Equation (6)

$$-2\pi f\tau_{n+1,n} = \tan^{-1}\left(\frac{2\omega C G_{ant}}{G_{ant}^2 - \omega^2 C^2}\right),$$

and therefore

$$\tau_{n+1,n} = -\frac{1}{2\pi f}tan^{-1}\left(\frac{2\omega C G_{ant}}{G_{ant}^2 - \omega^2 C^2}\right). \tag{10}$$

Moreover, one can also derive the relationship between the angle of the incoming signal (α) with the value of varactor by substituting Equation (10) to Equation (7)

$$\alpha = sin^{-1}\left(-\frac{c}{2\pi f d}tan^{-1}\left(\frac{2\omega C G_{ant}}{G_{ant}^2 - \omega^2 C^2}\right)\right). \tag{11}$$

From Equation (11), we can find the suitable varactor value (C) given the angle of an incoming visible light signal. To find the value of varactor (C) we can implement the non-linear optimization technique defined as follows:

$$\min_{C}\left(\alpha - \sin^{-1}\left(-\frac{c}{\omega d}\tan^{-1}\left(\frac{2\omega C G_{ant}}{G_{ant}^2 - \omega^2 C^2}\right)\right)\right)^2, \tag{12}$$

subject to the constraint of minimum and maximum of the tunable value of varactor $C_{min} \le C \le C_{max}$.

The proposed method can be observed in the flowchart in Figure 4.

TABLE I
THE NOMINAL PARAMETERS OF THE SIMULATION

Symbol	Parameter	Value	Unit
c	Speed of light	3×10^8	m/s
G_{ant}	Antenna gain	80	dB
f	Frequency of the light signal	500	THz
d	Distance between antenna/sensor	1×10^{-2}	m
C_{min}	The minimum value of tunable varactor	4	pF
C_{max}	The maximum value of tunable varactor	20	pF

*) We assume that the varactors and transmission lines were assumed to be lossless.

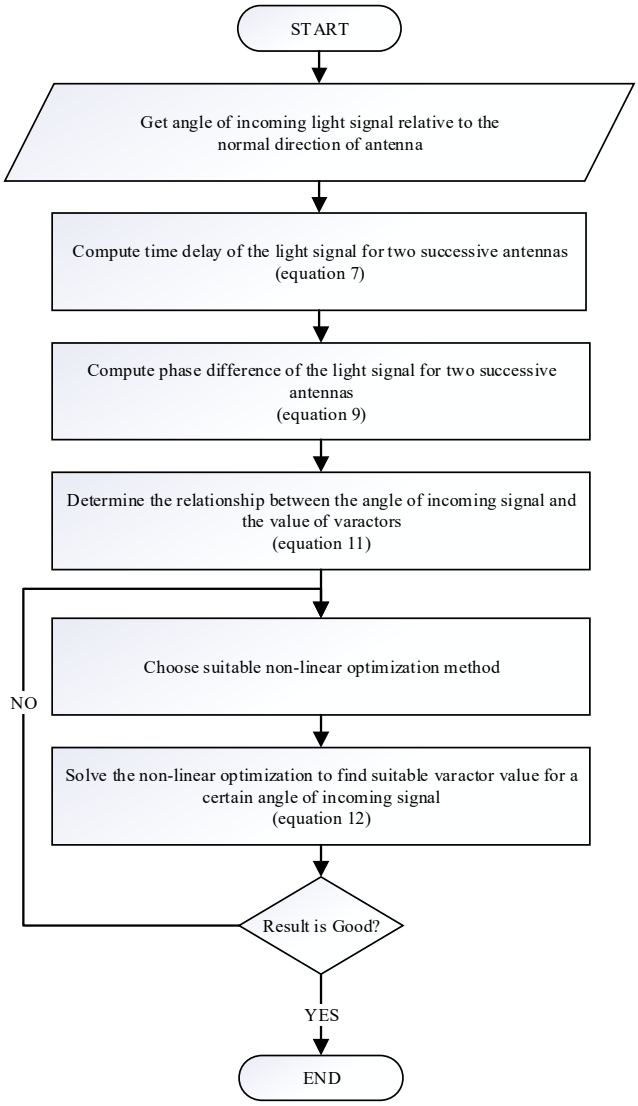

Fig. 4 The flowchart of the proposed method for tuning of extended resonance based beamforming system

III. Result and Discussion

A. Simulation Setups

The nominal parameters of setup simulation in this paper are shown in Table 1. The angle of the incoming light signals is given. The phase difference between the signal received by each sensor can be calculated from the given incoming angles. It is assumed that the varactors and transmission lines are lossless. The value of the varactor is obtained by solving the optimization problem stated in Equation (12). That optimization problem is non-linear optimization problem with constraints.

B. Simulation Results

The simulation was performed in MATLAB using the optimization toolbox for non-linear optimization with constraints, i.e., fmincon. The optimization algorithms which will be used are active set [19], interior point [20], and sequential quadratic programming (SQP) [21]–[23]. The simulation result for some phase difference values is presented in **Error! Reference source not found.**. It is clearly shown in Figure 5 that all three optimization algorithms used in this simulation work well for small phase differences, e.g., $\pi/12$ and $\pi/4$. However, when the phase difference is $\pi/2$, all three algorithms fail to produce function value that approaces zero.

It is interesting to simulate other phase differences and observe which phase difference. All three algorithms fail to produce good varactor value. The simulation was performed for the additional phase difference $\pi/6$ and $\pi/3$. The result of the simulation is presented in Fig. 5 Simulation results for some different values of phase difference: (a) $\pi/12$, (b) $\pi/4$, and (c) $\pi/2$.

TABLE. It is confirmed that only $\pi/2$ phase difference has big final function value.

One can observe from Fig. 5 Simulation results for some different values of phase difference: (a) $\pi/12$, (b) $\pi/4$, and (c) $\pi/2$.

TABLE that the optimization process hits the constraint barrier when the phase difference is $\pi/2$. Indeed, as mentioned in

TABLE I, the value of varactor is from $C_{min} = 4$ pF, and $C_{max} = 20$ pF, or the tunability of the varactor is 5:1. Figure 6 (left) shows the relationship between the varactor tunability to the maximum phase shift. When the varactor tunability is equal to 5:1, the maximum phase shift can be observed is only 83,6206 degrees.

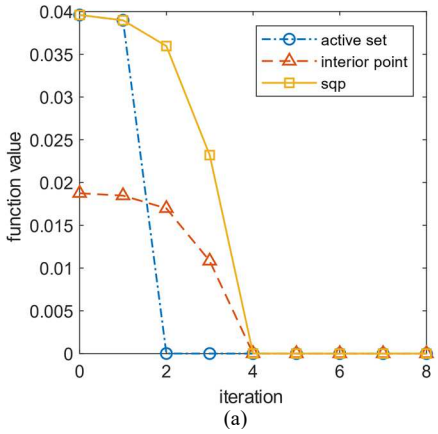

(a)

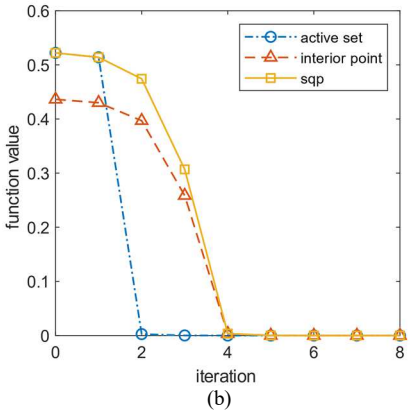

(b)

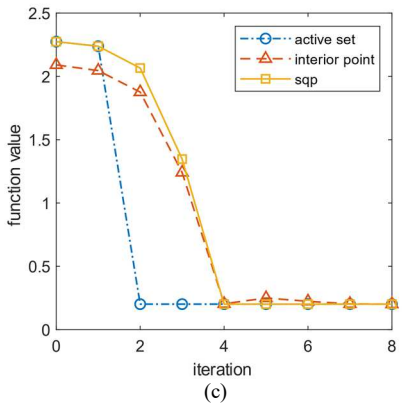

Fig. 5 Simulation results for some different values of phase difference: (a) $\pi/12$, (b) $\pi/4$, and (c) $\pi/2$.

TABLE II
THE OBTAINED VALUE OF VARACTOR FOR A DIFFERENT PHASE DIFFERENCE.

No	Target phase difference (degree)	Tuned value of varactor (pF)	Final function value
1.	$\pi/12$	4.1906	3.943531×10^{-18}
2.	$\pi/6$	8.5291	1.387785×10^{-17}
3.	$\pi/4$	13.1848	3.031748×10^{-17}
4.	$\pi/3$	18.3776	4.190854×10^{-17}
5.	$\pi/2$	20.0000	2.014502×10^{-1}

Therefore, we can observe a limitation in the flexibility of the varactor. An interesting question now arises: how can we determine the required varactor tunability needed to a certain value of phase differences? Figure 6 shows the relationship between varactor tunability values and the maximum phase difference it can handle for a visible light wave frequency range. If we want to achieve $\pi/2$ phase difference, then we should use a varactor with tunability of more than 10:1. The higher the tunability, the higher the phase difference it can handle.

However, there is still a limitation: when the tunability is already very high, a significant increase of the tunability will not significantly increase the maximum phase difference. This can be observed when we are comparing tunability 30:1 and 50:1. There is no significant difference in the maximum phase they can produce, especially in the lower frequency region.

Figure 7 shows the array factor for the five-photodetectors used as a visible light sensor for VLC. One can observe that the obtained varactor value can create a phase shift that results in a shift of the array factor, as long as the tunability of the varactor is more than enough to handle the phase difference. In order to confirm that the phase-shifting obtained from the extended-resonance-based beamforming system is indeed enough to compensate the phase difference in the five-photodetectors, we create the polar plot of the array factor pattern. As we can observe in Figure 8, for each photodetector, the obtained phase shift compensates the phase difference in each sensor, resulting in the phase of all sensors will be in phase.

From Figure 8 (a), we see that since the first antenna is considered the reference phase, the phase difference is 0, no extra phase shift is needed, i.e., phase shift from extended-resonance beamformer equals 0. From Figure 8 (b-e), we can clearly observe some phase differences between the particular antenna and the first antenna. This phase difference should be corrected by the phase shift provided by the extended resonance beamformer.

We can also see that for each image in Figure 8 (b-e), the phase shift provided by the beamformer can compensate for the phase difference. If we add the phase difference and the phase shift, the resulting phase will be 0, or in other words, all of the antennas are in phase, so the signals received by all antennas are constructive to each other. This proves that the proposed method can find the suitable varactor values of the beamformer.

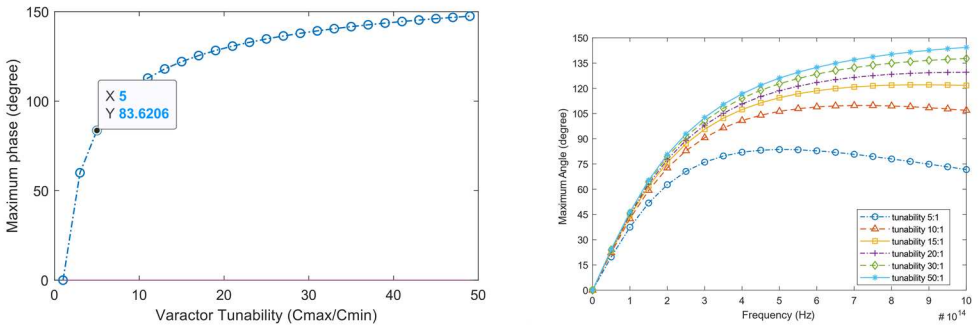

Fig. 6 (left) - Maximum phase difference can be achieved for a different value of varactor tunability (C_{max}/C_{min}). (right) - Maximum phase difference can be achieved as a function of frequency for a different value of varactor tunability.

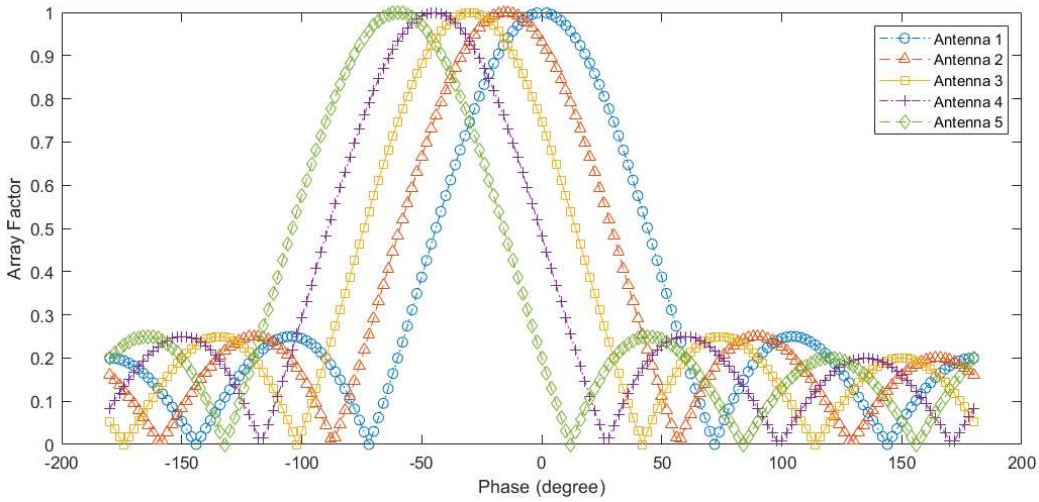

Fig. 7 The array factor for the five-photodetectors signals.

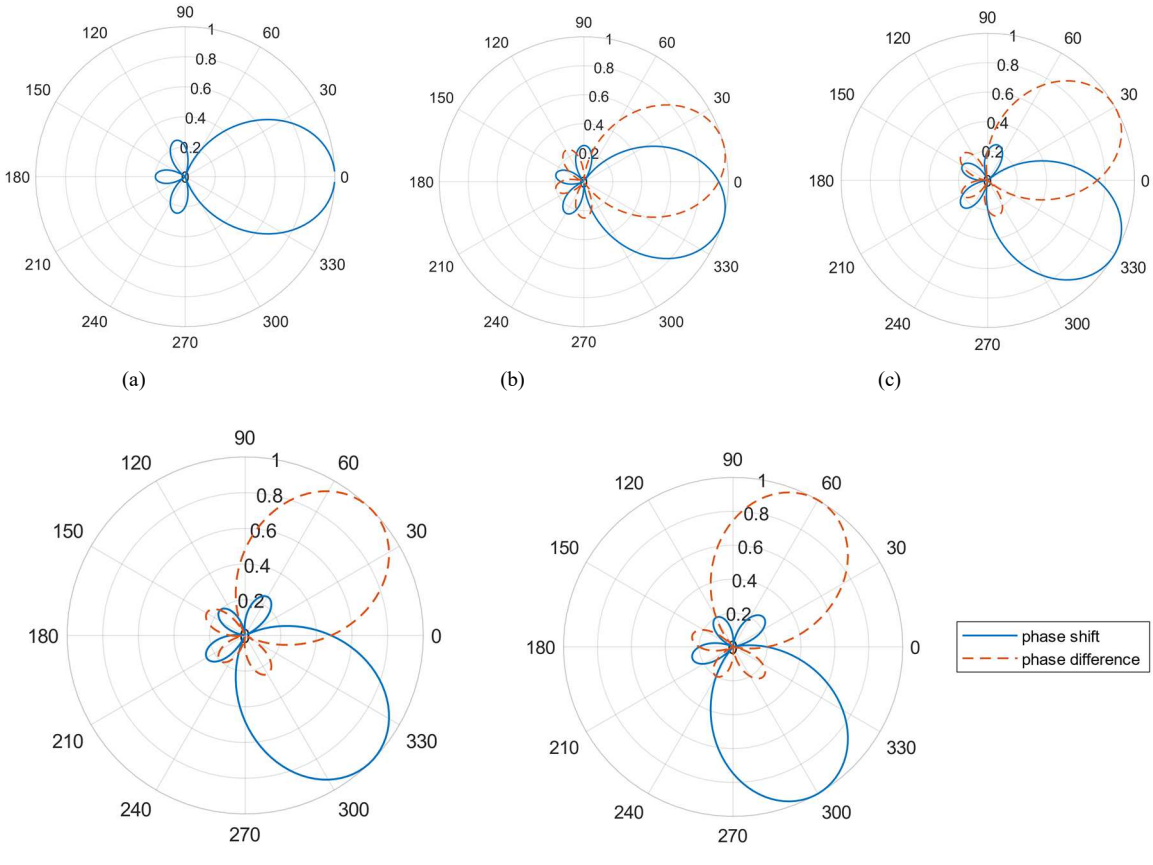

Fig. 8 The array factor pattern for each of the five-photodetectors. Each phase-shifting obtained from an extended-resonance-based beamforming system compensates the phase difference. (a) antenna 1, (b) antenna 2, (c) antenna 3, (d) antenna 4, and (e) antenna 5.

IV. Conclusions

The extended-resonance-based beamforming system can produce phase shifting enough to compensate for the phase difference from the signal received by each photodetector. We should make sure that the tunability of the varactor used in the beamformer is enough to compensate for a required phase difference. Given that the varactor is chosen carefully and sufficient, the non-linear optimization method such as active set, interior point, or sequential quadratic programming can tune the varactor so that the beamformer will compensate for the phase difference from the incoming signal.

Acknowledgment

This research was funded by Directorate of Research and Community Service, Directorate General of Research and Development Strengthening, Ministry of Research,

Technology, and Higher Education, Republic of Indonesia, with Research Contract Number: 109/SP2H/LT/DRPM/2019.

REFERENCES

[1] N. Consulting, "Energy Savings Forecast of Solid-State Lighting in General Illumination Applications," *U.S. Dep. Energy Rep.*, no. August, pp. 2013–2014, 2014.

[2] Y. Tanaka, S. Haruyama, and M. Nakagawa, "Wireless optical trasnsmissions with white colored LED for wireless home links," *IEEE Int. Symp. Pers. Indoor Mob. Radio Commun. PIMRC*, vol. 2, pp. 1325–1329, 2000, doi: 10.1109/pimrc.2000.881634.

[3] T. Deepa, H. Mathur, and K. A. Sunitha, "Spectrally efficient multicarrier modulation system for visible light communication," *Int. J. Electr. Comput. Eng.*, vol. 9, no. 2, p. 1184, 2019, doi: 10.11591/ijece.v9i2.pp1184-1190.

[4] P. H. Pathak, X. Feng, P. Hu, and P. Mohapatra, "Visible Light Communication, Networking, and Sensing: A Survey, Potential and Challenges," *IEEE Commun. Surv. Tutorials*, vol. 17, no. 4, pp. 2047–2077, 2015, doi: 10.1109/COMST.2015.2476474.

[5] S. Cho, G. Chen, and J. P. Coon, "Securing visible light communication systems by beamforming in the presence of randomly distributed eavesdroppers," *IEEE Trans. Wirel. Commun.*, vol. 17, no. 5, pp. 2918–2931, 2018.

[6] S. U. Rehman, S. Ullah, P. H. J. Chong, S. Yongchareon, and D. Komosny, "Visible light communication: a system perspective—overview and challenges," *Sensors*, vol. 19, no. 5, p. 1153, 2019.

[7] C. Danakis, M. Afgani, G. Povey, I. Underwood, and H. Haas, "Using a CMOS camera sensor for visible light communication," *2012 IEEE Globecom Work. GC Wkshps 2012*, pp. 1244–1248, 2012, doi: 10.1109/GLOCOMW.2012.6477759.

[8] T. H. Do and M. Yoo, "Visible light communication-based vehicle-to-vehicle tracking using CMOS camera," *IEEE Access*, vol. 7, pp. 7218–7227, 2019.

[9] K. L. Hsu *et al.*, "CMOS camera based visible light communication (VLC) using grayscale value distribution and machine learning algorithm," *Opt. Express*, vol. 28, no. 2, pp. 2427–2432, 2020.

[10] H. Nugroho, W. K. Wibowo, A. R. Annisa, and H. M. Rosalinda, "Deep learning for tuning Optical Beamforming Networks," *Telkomnika (Telecommunication Comput. Electron. Control.*, vol. 16, no. 4, 2018, doi: 10.12928/TELKOMNIKA.v16i4.8176.

[11] H. Nugroho, "Tuning of Optical Beamforming Networks: A Deep Learning Approach." 2015.

[12] A. Meijerink *et al.*, "Phased Array Antenna Steering using a Ring Resonator-based Optical Beam Forming Network," in *Proceedings of the IEEE Symposium on Communications and Vehicular Technology*, Nov. 2006, pp. 7–12.

[13] H. Schippers *et al.*, "Broadband Conformal Phased Array with Optical Beamforming for Airborne Satellite Communication," in *Proceedings of the 2008 IEEE Aerospace Conference*, Mar. 2008, pp. 1–17.

[14] M. Elhefnawy, "Design and simulation of an analog beamforming phased array antenna," *Int. J. Electr. Comput. Eng.*, vol. 10, no. 2, pp. 1398–1405, 2020, doi: 10.11591/ijece.v10i2.pp1398-1405.

[15] R. Maneiro-Catoira, J. Brégains, J. A. Garc\'\ia-Naya, and L. Castedo, "Analog beamforming using time-modulated arrays with digitally preprocessed rectangular sequences," *IEEE Antennas Wirel. Propag. Lett.*, vol. 17, no. 3, pp. 497–500, 2018.

[16] Y. Ding, V. Fusco, A. Shitvov, Y. Xiao, and H. Li, "Beam index modulation wireless communication with analog beamforming," *IEEE Trans. Veh. Technol.*, vol. 67, no. 7, pp. 6340–6354, 2018.

[17] D. G. Rabus, *Integrated Ring Resonators: The Compendium*. Berlin, Heidelberg: Springer, 2007.

[18] A. Tombak and A. Mortazawi, "A Novel Low-Cost Beam-Steering Technique Based on the Extended-Resonance Power-Dividing Method," *IEEE Trans. Microw. Theory Tech.*, vol. 52, no. 2, pp. 664–670, 2004, doi: 10.1109/TMTT.2003.822031.

[19] R. H. Byrd, N. I. M. Gould, J. Nocedal, and R. A. Waltz, "An algorithm for nonlinear optimization using linear programming and equality constrained subproblems," *Math. Program.*, vol. 100, no. 1, pp. 27–48, 2004, doi: 10.1007/s10107-003-0485-4.

[20] A. Wächter, "An Interior Point Algorithm for Large-Scale Nonlinear Optimization with Applications in Process Engineering," *PhD thesis*, 2002.

[21] P. T. Boggs and J. W. Tolle, "Sequential quadratic programming for large-scale nonlinear optimization," *J. Comput. Appl. Math.*, vol. 124, no. 1–2, pp. 123–137, 2000, doi: 10.1016/S0377-0427(00)00429-5.

[22] O. D. Montoya, W. Gil-González, and A. Garces, "Sequential quadratic programming models for solving the OPF problem in DC grids," *Electr. Power Syst. Res.*, vol. 169, pp. 18–23, 2019.

[23] A. Mehmood, A. Zameer, S. H. Ling, A. ur Rehman, and M. A. Z. Raja, "Integrated computational intelligent paradigm for nonlinear electric circuit models using neural networks, genetic algorithms and sequential quadratic programming," *Neural Comput. Appl.*, vol. 32, no. 14, pp. 10337–10357, 2020.